



Design, Fabrication and Testing of a SEPIC DC-DC Converter for Interfacing Solar PV Module

Gwani Mohammed^{1*} | Bako Abdullahi^{1,2} | Umar Muhammad Kangiwa¹ | Gado Abubakar Abubakar¹

¹Department of Physics, Faculty of Physical Sciences, Kebbi State University of Science and Technology, P.M.B 1144, Birnin Kebbi

²Federal University Birnin Kebbi. P. M. B 1157 Birnin Kebbi

*Corresponding Author Address/Phone No.: gwanimohammed@gmail.com/+2348032791889

To Cite this Article

Gwani Mohammed, Bako Abdullahi, Umar Muhammad Kangiwa and Gado Abubakar Abubakar. Design, Fabrication and Testing of a SEPIC DC-DC Converter for Interfacing Solar PV Module. *International Journal for Modern Trends in Science and Technology* 2022, 8 pp. 269-277. <https://doi.org/10.46501/IJMTST0801047>

Article Info

Received: 12 December 2021; Accepted: 10 January 2022; Published: 14 January 2022.

ABSTRACT

Renewable energy resources utilization could be a feasible solution for mitigating the problem of power supply due to energy imbalance between the demand and generation in the nation. Solar energy resource is abundantly available but its exploitation through PV system is not economically feasible. In order to optimize the power output and reduces the cost, an electronics device should be integrated with solar PV system. A high classical 10 V / 60 V DC-DC SEPIC converters for renewable energy an application was designed constructed and tested. The converter was designed through simulation using Multisim software (13.0.0) tools. The system was tested by integration with 20 W PV modules while exposing the PV module to sun radiation. The effects of input parameters such as sun radiation and other useful power inputs on PV module and a DC-DC power converter outputs were investigated. The simulation results showed that 61.6 V was achieved by the converter with 83.36 % voltage regulation and 10.88 dB voltage gains.

KEYWORDS: DC-DC converter, Photovoltaic (PV) Panel, Single switch, High step-up voltage gain, Duty cycle

1. INTRODUCTION

Today's global energy supply mainly comes from fossil fuels such as coal, oil and natural gas which are major sources of greenhouse gases. The Earth's climate will be jeopardized if we continue depending on these fuels without scalable replacements [7]. The current energy system is unsustainable; it needs a transformation to a sustainable global energy supply system. It is also regarded as an influential parameter of fiscal and societal prospective; no country has developed without ensuring least contact to energy resources beyond a survival economy for a wide section of its populace [10][11].

Solar energy production is clean, emission-free with continuous supply during the day while being portable and scalable. Moreover, photovoltaic system is the process of converting sunlight directly into electricity using solar cells in two phases. In the first phase, solar radiations are absorbed within the semiconductor while in the second phase current/voltage is generated due to the production of electrons-hole pairs by the incident radiation[10][3].

In this period of energy crisis researchers in the field of renewable energy resources are gaining more considerable momentum [1][2]. Renewable energy is energy generated from natural resources such as

sunlight, wind, tides and geothermal heat which are renewable (naturally replenished) [9]. A non-renewable resource is a limited natural resource that cannot be re-made or re-grown in a short amount of time [5][14].

1.1 Solar Energy

Solar and wind power are the most common sources of renewable energy, Recently, there has been a rapid increase in the use of the energy resources, due to the depletion of fossil fuels and environmental pollutions, solar energy is natural, inexhaustible, clean, free of charge, less ecological pollution and with modular character which allows the construction of the solar array at different power levels [3][6].

Power Converter can be essentially divided into either DC-DC or DC-AC types. The DC-DC deal with stepping up the DC voltage generated from the PV panel while the other one deal with conversion of DC to AC signal for inverter application. DC-DC Converter in many technical applications, it is required to convert a set DC voltage source into a variable-voltage DC output [13][12].

Most of the research works are channeled toward solar and wind energy being them common among the available renewable energy resources. The sun and wind are virtually inexhaustible energy resources, the ability to harness the energy and convert it to electricity for consumption will result in solving most of our energy predicaments [4][8]. A novel high step-up DC-DC converter for PV application was proposed in [7] but the converter has too much components in it, as such the converter too expensive. [10] Reported an integrated double boost-sepic DC-DC converter for fuel cell and PV applications, the topology has a large duty-cycle which can easily caused stress within the components. The topology reported in [8] has high gain and low duty-cycle but its switching voltage is equals to twice the input voltage which is not expected to make the switch works properly and resulted in high stress within the component.

In this paper, a simple SEPIC converter was combined with a voltage multiplier cell to design a SEPIC DC-DC converter for interfacing PV module applications. The proposed converter implored a single switch for switching control. The advantages of the topology are: cheap, light, less stress across the semiconductor devices, and high voltage gain. This DC-DC converter will boost any input of 10 V DC

voltages to an output of 60 V DC voltages as shown in Figure 1. Verification of the performance of the converter was done by simulation and prototype circuit was later developed and tested in the laboratory.

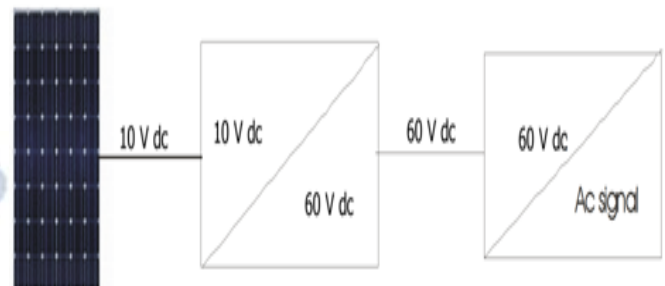


Figure 1: Graphical representation of the proposed converter system.

2.0 MATERIALS AND METHODS

2.1 Materials

The materials used for the design, construction and performance analysis of DC-DC SEPIC Converter for solar PV systems

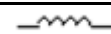
The measuring instrument used for the DC-DC SEPIC converter performance investigation is short-listed in Table 1.

Table 1: Measuring Instruments

Instrument	Specifications
Pyronometer	TES 1333R Data logging Solar power meter
Multimeter	DT9205A, DT-830D and DT9201A (0 – 120 V)
Oscilloscope	CA6620 20MHz
Variable power supply	MCR – 303A DC POWER SUPPLY

Electronics devices used for the construction of the DC-DC SEPIC converter are shown in Table 2.

Table 2: Electronics devices used

Devices	Variables	Unit
Inductors		2, L ₁ & L ₂
Signal generator		1 MOSFET
Diodes		3, D ₁ , D ₂ , & D ₃
Capacitors		3, C ₁ , C ₂ & C ₃

The specification of the 20 W module used in this research is shown in Table 3

Table 3: Solar PV Module specifications

Maximum power (Pmax)	20W
Output Tolerance	±5%
Current at Pmax (Imp)	1.14A
Voltage at Pmax (Vmp)	17.5V
Short- circuited current (Isc)	1.27 A
Open- circuited Voltage (Voc)	22.05 V
Maximum system voltage suitable for the PVPanel DC	12 V
Module Dimension (m ²)	(0.1645 m ²)

2.2 Methods

The methods Adopted for the design and Experimental Test of the DC-DC SEPIC converter are presented.

The proposed circuit diagram of the DC-DC SEPIC Converter consists of a power input source, 2 Inductors, and 1 signal generator, 3 diodes, 3 capacitors, Figure 4 present a circuit diagram of the proposed SEPIC converter. The square wave supplied to the MOSFET through the source and the MOSFET switched the system into actions by raising the output voltage to 30 V. The simulation was conducted with 10 V input and the system was run for about 1.071500 transitions until the output voltage was approximately 60 V. Though, simulation was conducted several times under varying time conditions. In each case, the output voltage was recorded and the average voltage was evaluated.

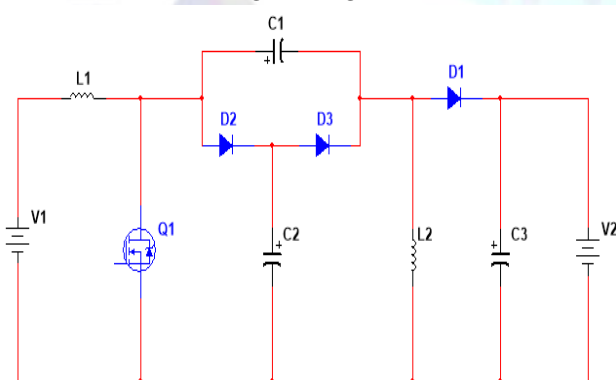


Figure 2: Circuit diagram of the proposed SEPIC converter

Design Equation of DC-DC SEPIC converter

The propose design equations was used and evaluated. Highlight of some of the equations that would be used to calculate the parameters mention in Table 2: it can be seen that, the proposed converter is a product of classical boost converter integrated together in cascade arrangement. Therefore, the theoretical analysis can be obtained from the circuit above (Figure 2) as:

$$V_{in} = V_{L1} \tag{1}$$

$$V_{C3} = V_{output} = V_{C1} + V_{C2} \tag{2}$$

$$V_{in}d = (V_{C2} - V_{in})(1 - d) \tag{3}$$

$$V_{in}d = V_{C2} - V_0d - V_{in} + V_{in}d \tag{4}$$

$$V_0 = \left(\frac{V_{in}}{1-d}\right) \tag{5}$$

$$\frac{V_0}{v_{in}} = \left(\frac{1}{1-d}\right) \tag{6}$$

C_1, C_2, D_1 & D_2 are representing voltage doubler, and M is representing the number doubler circuit used. Hence in this project one voltage doubler circuit is used and therefore $M = 1$

Now equation will take the form

$$\frac{V_0}{V_{in}} = \left(\frac{M+1}{1-d}\right) \tag{7}$$

Where $\frac{V_0}{V_{in}}$ are voltage gain, M is the number of voltage multiplier cell used and V_0 voltage output

$$\frac{V_0}{V_{in}} = \left(\frac{2}{1-d}\right) \tag{8}$$

In terms of duty cycle equation 9 will take the form

$$2V_{in} = V_0 - V_0d \tag{9}$$

The value of duty-cycle of the switching signal will be calculated using, equation (10)

$$d = \frac{V_0 - V_{in}(m+1)}{V_0} \tag{10}$$

In terms of voltage from equation 8

$$\frac{V_0}{V_{in}} = \text{gain} = \left(\frac{2}{1-d}\right) \tag{11}$$

In terms of voltage stress on switch, the voltage stress of the components will be calculated using, equation (16)

$$V_{switc h} = v_{in} \left(\frac{1}{(1-d)}\right) \tag{12}$$

Where V_{in} is the voltage input, and d is the duty cycle

3.0 SIMULATION

The designed circuit diagram of the 10V / 60 V DC-DC SEPIC converter with the actual sizes number of electronics components as shown in Figure 2 is presented on Multism version 13.0.0 for simulation. The components sizes were selected from the datasheet and the system was run for simulation. The topology was built by incorporating voltage multiplier cells in a conventional boost converter to test the presented topology. The voltage multiplier cell contains 2 capacitors and two diodes were introduce, this

determined complete proposed DC-DC SEPIC converter with 60V DC as the output voltage of any input voltages ranges within the 6 V – 10 V as input voltages. In the simulation, the system was triggered by the square wave AC pulse of 10 V magnitude 1KHZ frequencies. The simulations results and complete circuit were physically determined by running the circuit design as illustrated in Figure (3 & 4).

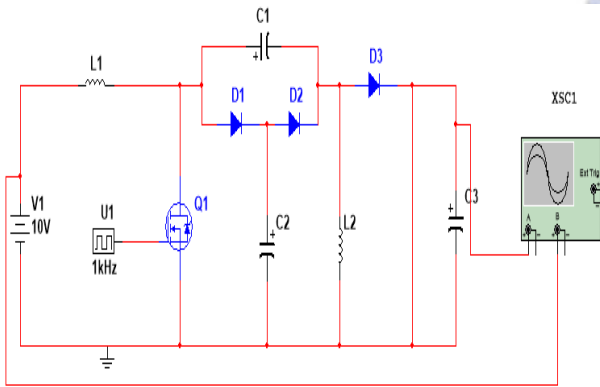


Figure 3: The Proposed DC-DC SEPIC Converter output voltage Topology

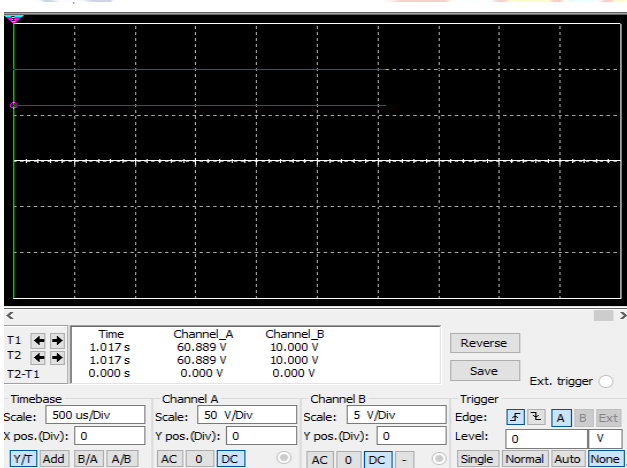
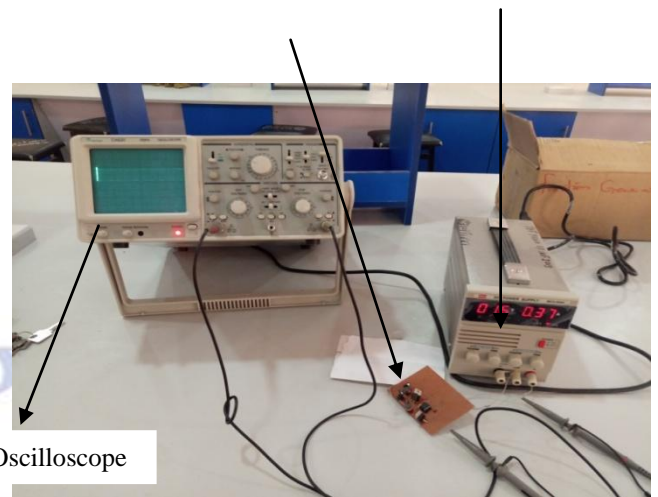


Figure 4: Complete circuit simulations results via multisim

3.1 Testing of DC-DC SEPIC converter

3.1.0 Hardware Test

The DC-DC SEPIC converter was tested; the input terminals of the converter were connected to the DC source through a variable DC power supply system, while the output terminals were connected to the oscilloscope. The 10 V DC power was selected from the DC power supply, while the output DC voltage was monitored through the oscilloscope. The output voltage with the respect to time and its amplitude was monitored and recorded from the oscilloscope. Figure 5. Shows a DC-DC converter interconnection between the DC power supply and oscilloscope



Oscilloscope

Figure 5: The DC-DC converter hardware test

3.2 Experimental Tests

The outputs of the PV module were connected to the two digital multimeter which serve as the input voltage to the converter were measured and recorded. The direct sun radiation striking the surface area of the PV module has been measured simultaneously with the input and output voltages at intervals of 10 minutes. These data were collected for 10 days and average hourly results were obtained. The experimental set up of DC-DC SEPIC converter consisting of stands tools, PV module, constructed system and two Multimeter are shown in Figure 6.



Figure 6: Experimental set up of DC-DC converter

4.0 RESULTS AND DISCUSSION

Results of the simulation and Test analysis of 10V-60V DC-DC SEPIC converter. The theoretical equations and list of the parameters used which include the respected value of the proposed converter are analyze while the

voltage across all the component was determined and indicated in Figure 7 to 20 and the testing results were presented in Figure 21 and 22.

The schematic diagram for the choice of the inductor on mutism software is shown in Figure 5; and the $10 \mu\text{H}$, 10 V inductor was found to be suitable from the Mutisim. The output of the simulated results obtained from multisim software as presented in Figure 7.

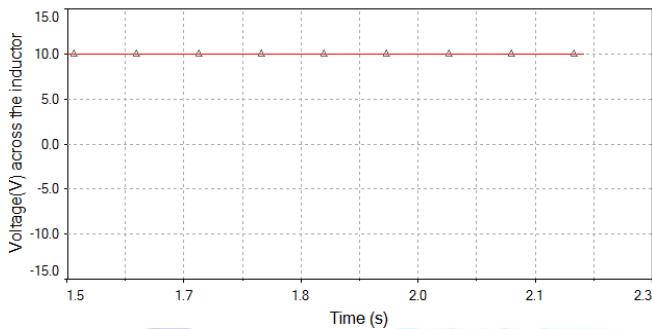


Figure 7: Output voltage graph across the Inductor L_1 . The input of the MOSFET is connected to the output of the inductor L_1 which is $10 \mu\text{H}$, 10 V as shown in Figure 8. The MOSFET of voltages ranges from 3.8 V to 32 V which corresponds to IRFZ44 were selected from the multisim data sheets and runs the output voltage was of 31.84 V .

The simulation result was indicated to view the input and output voltages in Figure 8. The pulse voltage signal is in form of the square wave which originally from the Multisim.



Figure 8: Output voltage graph across the switch (MOSFET)

The voltage doubler comprises, capacitor C_1 and C_2 diodes D_1 and D_2 as in the circuit diagram shown in Figure 2. The 31.848 V output voltage from the MOSFET is doubled by charging and discharging actions of capacitors C_1 and C_2 through the diode D_1 and D_2 . The capacitors 30 V were selected from the datasheet and the accurate outputs were obtained at approximately 60 V output. The capacitors sizes for C_1 and C_2 is $2.2 \mu\text{F}$ each. Similarly, the Diodes D_1 and D_2

with voltage ranges 50 V to 100 V with ranges from MUR105 to MUR110 were also selected and the Multisim was run the output voltage to the nearest value of 60 V . as indicated in Figure 9 to 12.

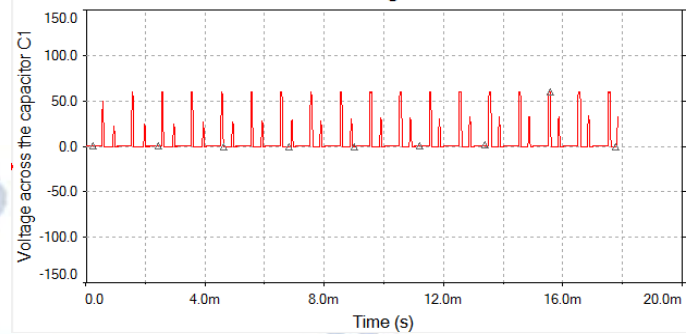


Figure 9: Output voltage graph across the capacitor C_1 (voltage doubler output)

The capacitor C_2 gives the voltage output as 27.87 V . When the voltage through the two branches of the doubler was summed, the total output gives 60.893 volts which is approximately the required output voltage for the DC-DC SEPIC converter as in Figure 10.

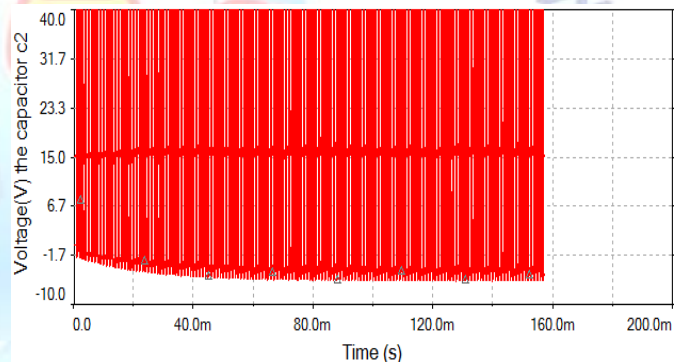


Figure 10: Output voltage graph across the capacitor C_2 . The output voltage doubler gives 60.893 which has to drop across the inductor L_2 , the inductor with voltage ranges from 36.0 V to 64.5 V of inductances $250 \mu\text{H}$ were selected from datasheet and the output voltage shows the reduction to 60.31 V as shown in Figure 11.

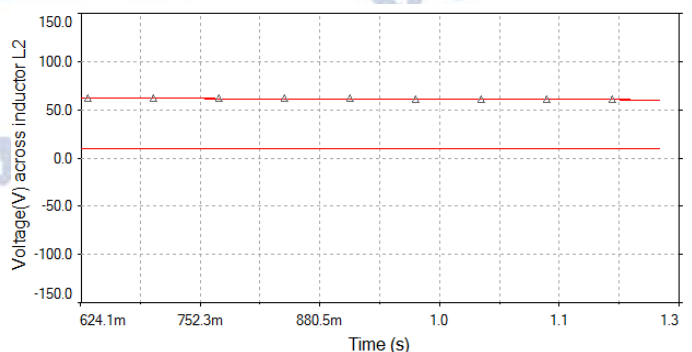


Figure 11: Output voltage graph across the Inductor L_2 . The diodes with voltage ranges from 50 V to 100 V could accept the output voltage of the inductor (60.316

V). The diodes MUR110 were also selected from datasheet and gives 60.624 V output. The simulation result shown in Figure 12. Indicates the diode D₃ will rectify the voltage ripples from AC to DC.

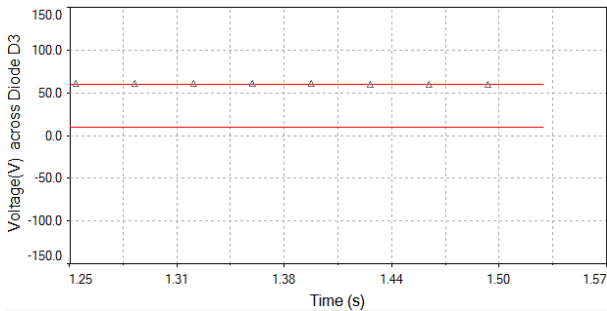


Figure 12: Output voltage graph across the Diodes D₃. The capacitor C₃ with voltage ranges 50 V - 60 V of the capacitance 0.47 μ F to 10 μ F were selected from data sheet while running the simulation the output as exactly 60 V. The capacitor of capacitance 2.2 μ F was suitable. The simulation result of the output capacitor C₃ is shown in Figure 13.

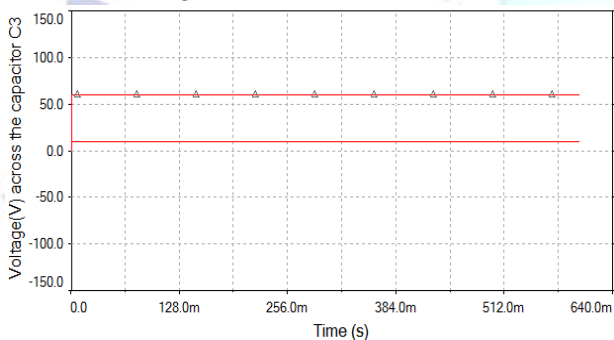


Figure 13: Output voltage graph across the capacitor C₃. Results of the simulation of 10 V - 60 V DC-DC SEPIC converter presents a graph of Input and average output voltages of DC-DC converter against percentage voltage regulations. The result shows that the DC-DC converter voltage output was 61.6 V enhancing percentage regulations of 83.6%. Moreover, as the simulation was run from 10.0 seconds to 34.0 seconds at fixed 10 V input, this means that DC-DC converter voltage regulation is directly proportional to the difference between the output and input voltages but inversely proportional to the output voltage as from Figure 14. This indicated that about 80 % of the input voltage which is 8 V has been regulated by the converter to generate 48 V. Similarly, Figure 15 presents a graph of average input and average output voltages of DC-DC Converter Voltage gain (dB), the result shows that the DC-DC converter voltage gain was 14.93 (dB) enhancing DC-DC converter voltage output of 61.6 V. However, the DC-DC converter voltage output and

gain maintained stable values of 50.7 V and 14.11 dB respectively.

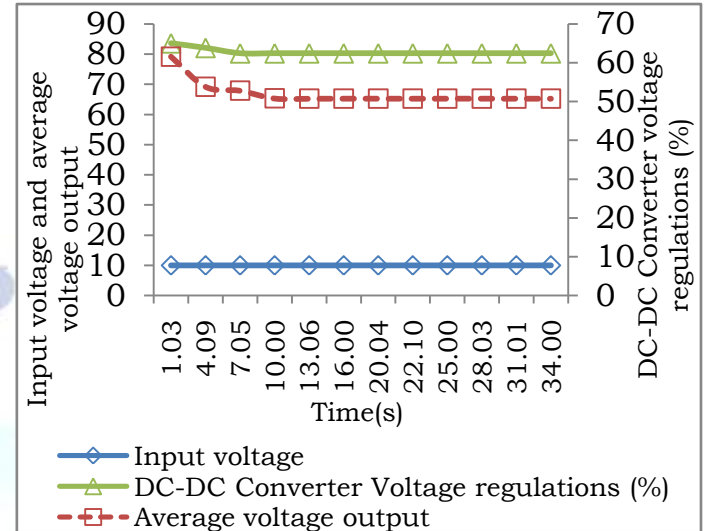


Figure 14: Input and output Voltages of DC-DC Converter against Voltage Percentage Regulations

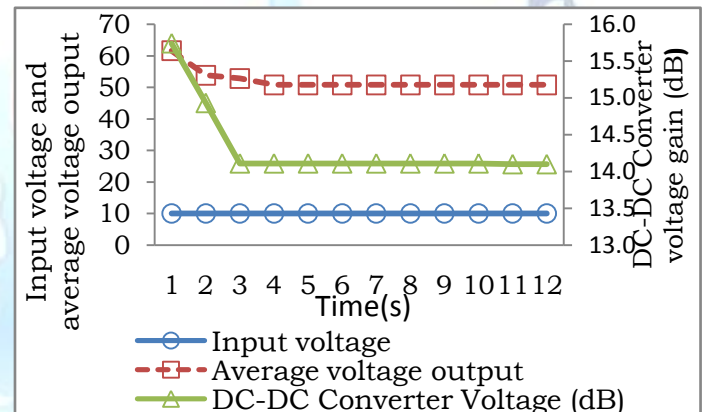


Figure 15: Input voltages and output voltage of DC-DC converter Vs Voltage gain(dB)

4.1 Experimental Test Results for the DC-DC SEPIC Converter

Figure 16 presents a graph of the correlation between the PV module and DC-DC converter output voltages against DC-DC converter voltage regulation. The result shows that at the peak DC-DC converter percentage voltage regulation of 52.04 % was obtained by 12:00 pm, when the PV module and DC-DC converter output voltages are 13.15 V and 27.42 V respectively. The percentage voltage regulation has drifted suddenly to 46.14 % at 3:00 pm, and later rose up to 52.3 % at 5:00 pm. During this period, both the PV module and DC-DC converter voltage outputs are simultaneously decreasing. This indicated that the percentage voltage regulation of the DC-DC converter depends more on its output voltage than the PV module output.

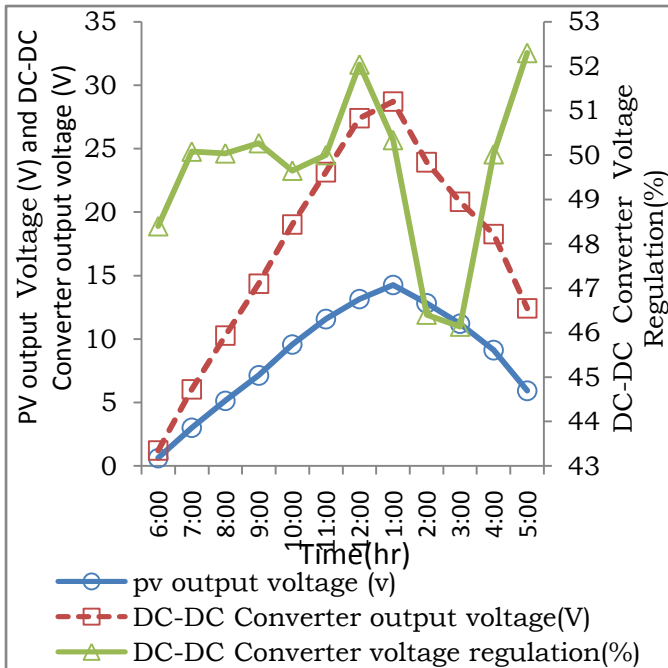


Figure 16: Graph of correlation between the PV output voltage, DC-DC Converter output voltage, and DC-DC converter voltage regulation

Figure 17 presents a the correlation between the PV output voltages and DC-DC converter output voltage against DC-DC converter voltage gain, the result shows that around 1:00 pm the PV module reached a peak value of 14.23 V which had been converted to 28.71 V by the DC-DC converter voltage attaining voltage gain of 5.37dB. Moreover, a fluctuation in terms of voltage gain has been observed from 11:00 am to 5:00 pm, although the PV module and the DC-DC converter output voltages kept decreasing. However, the voltage gain has risen up to a maximum of 6.4 dB when the PV module and DC-DC converter have lower values of 5.292 V and 12.4 V respectively. This indicates that the voltage gain has no much correlation with the PV module and DC-DC converter output.

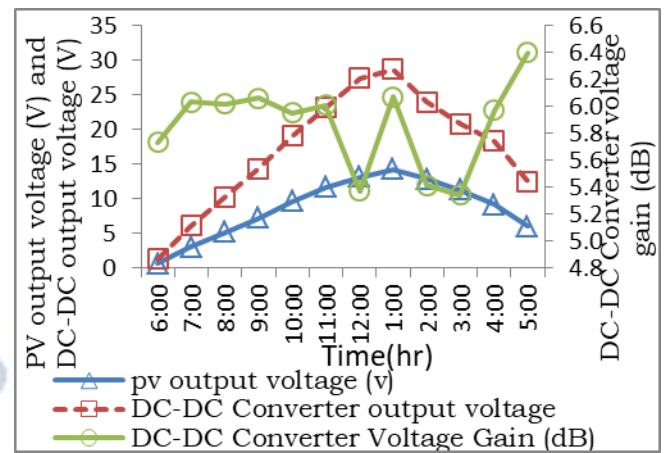


Figure 17: Graph of correlation between the PV output voltages, DC-DC Converter output voltage, and DC-DC converter voltage Gain

The results showed in Figure 18 presents a graph of correlation between the sun radiations and useful solar power input under no-load conditions. The results show that at maximum sun radiation of 971.13 W/m² was observed at around 12:00 pm which raised the useful solar power input to 159.48 W. Figure 17 presents graph of correlation between the useful solar power input and Solar PV power output under no-load conditions. The result shows that Solar PV modules generated 13.91 W when the useful solar power input has the maximum value of 159.4 W. This indicated that the solar PV module power output depends dully on the useful solar power input. So also it has been shown that both the useful solar power input and solar PV module power output followed the same trends.

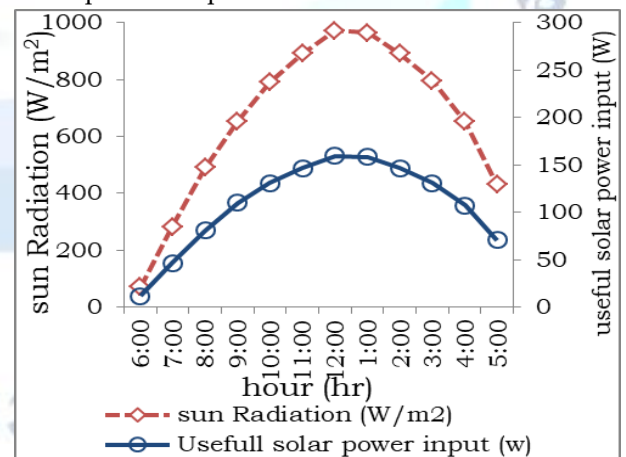


Figure 18: presents a graph of the Correlation between the Sun Radiation and Useful solar power input

4.2 DISCUSSION

The result of the DC/DC converter simulation from Figure 14 where 80.3% percentage voltage regulation of the converter remains steady at 50.81 V fixed. This means that about 80 % of the input voltage (8V) has been controlled by the converter to generate 48 V output enhancing the percentage voltage regulations of 83.6% as the simulation was run for 7.045 seconds. Similarly, the result of the voltage gain (dB) for the DC-DC converter showed in Figure 15 indicated that the voltage has reduced from 61.6 V to 53.81 V which is 12.6 %. This decrease in voltage was due to the increase in simulation time by 1 second, meaning that DC-DC converter gain responded to the time of simulation more than the input voltage. Consequently, the converter has attained its stable voltage gain of 14.1 dB when its output remains steady with 50.7 V which is 85.5 % of 60 V the input voltage.

The correlation between the sun radiation and useful input power been presented in Figure 18 showed that maximum average daily sun radiation of 971.31 W/m², the 20 W PV module of dimension 0.1645 m² has consequently captured 159.45 W useful input power which is 16.4 % for electricity generation. However, the raise and falling of the useful power input from morning to evening was due to the seasonal and periodic variability of sun radiation.

However, the maximum values of PV module outputs and efficiencies under these conditions were 13.79 W, 10.13 % and 9.78 W, 14.15% respectively. The result of the power output is on agreement with manufactures specifications in Table 3 who predicted 20 W PV power output at standard sun radiation of 1000 W/m². Meanwhile, Investigation showed that the DC-DC converter output voltage correlates with its percentage voltage regulation more than with PV module voltage output, as presented Figure 16. The DC-DC converter percentage voltage regulations were found to be 52.04, this result showed an improvement in terms of voltage regulation when compared with [2] who obtained maximum voltage regulation of 32.12 % for the constructed DC-DC converter. The results of the correlation between the PV module and DC-DC converter output voltages with DC-DC converter voltage gain (dB) have been presented from Figure 17. The result confirmed that maximum of 6.4 dB was achieved and the fluctuation of the gain was resulted

due to the ideal situation of the DC-DC converter. The gain obtained from the constructed SEPIC DC-DC converter is better than the gains obtained from [7][11] who obtained values of 6 dB and 5 dB respectively.

The results of the statistical analysis from Table 4.1 compared the percentage voltage regulation between the simulation (predicted), the higher value of 71.43 %, and that of DC-DC converter could be obtained up to 88.98 % of the predicted 80.33 % voltage regulation. This is because the current flows through the active components of the DC-DC converter. Moreover, the mean standard error for the simulation percentage voltage regulation of the DC-DC converter was compared. The reduction of the error due to the converter could enhance better performance and the paired mean difference between the simulation (predicted) values of percentage voltage regulation of the DC-DC converter were compared. It has been shown that both values of standard error mean difference and T-values reduce because the DC-DC converter produced significant values of output voltage. Meanwhile, the standard error means of the simulation, DC-DC converter voltage gain been compared and limited errors.

5.0 CONCLUSIONS

The 10 V / 60 V DC-DC SEPIC converter has been designed, constructed and experimentally tested by integrating it with 20 W solar PV module. The DC-DC converter simulation results predicted that 61.6 V output voltage could be achieved with 83.6% voltage regulation and enhanced gain of 14.1 dB. The percentage voltage regulation and voltage gain of DC-DC converter depends on its output voltage which in turn depends on PV module output voltage. The DC-DC converter as tested has achieved 88.98% and 77.17% of the predicted percentage voltage regulation and voltage gain respectively.

The statistical analysis proved that the data obtained were accurate and accepted the model with limited standard mean errors and minimal mean paired differences. Therefore, the SEPIC DC-DC converter could be a technically and economically feasible for integration with solar PV system for energy optimization.

REFERENCES

- [1] Ajami, A., Ardi, H., & Farakhor, A. A Novel High Step-up DC/DC Converter Based on Integrating Coupled Inductor and Switched-Capacitor Techniques for Renewable Energy Applications. *IEEE Transactions on Power Electronics*, 30(8), 2015 4255–4263. <https://doi.org/10.1109/TPEL.2014.2360495>
- [2] Ashok Kumar Donadi1, W. V. Jahnvi. PG Scholar, Department of Electrical and Electronics Engineering, Sree Vidyanikethan Engineering College, Tirupati, AP, India. Assistant Professor, Department of Electrical and Electronics Engineering, Sree Vidyanikethan Engineering College, 2019 Tirupati, AP, India.
- [3] Belkaid, A., Colak, I., & Isik, O. Photovoltaic maximum power point tracking under fast varying of solar radiation. *Applied Energy*, 179, 2016, 523–530. <https://doi.org/10.1016/j.apenergy.2016.07.034>
- [4] Darhmaoui, H., & Sheikh, N. Savonius Vertical Wind Turbine : Design, Simulation, and Physical. (published) M.Sc Dissertation, 2017, 44-70.
- [5] Dileep. Ga, S.N. Singhb. A Research Scholar, Alternate Hydro Energy Centre, Indian Institute of Technology, Roorkee, Uttarakhand 2017 247667,
- [6] Hassan Fathabadi(2016)Novel high-efficiency DC/DC boost converter for usein photovoltaic systems *Solar Energy*125, 22–31.
- [7] Isah, H., Sagagi, Y. M., & Bako, A. A Modified Boost-Boost High Gain DC-DC Converter for Photovoltaic (PV) Based Off-Grid Applications, *Nigerian Journal of Basic and Applied Sciences*, 27(2), (2019) 70–75. <https://doi.org/10.4314/njbas.v27i2.10>
- [8] Kanimozhi, G., Meenakshi, J., Vt, S., Andri, I., Kanimozhi, A. G., Meenakshi, J., & Vt, S. Small Signal Modeling of a DC-DC Type Double Boost Converter The Modeling Signal of a Type Double Boost Converter Integrated With SEPIC Converter Using State-Space Averaging Integrated With SEPIC Converter *EnergyProcedia*,117, 2017 835–846. <https://doi.org/10.1016/j.egypro.2017.05.201>
- [9] Kuo, Y. C., Huang, Y. M., & Liu, L. J. Integrated circuit and system design for renewable energy inverters. *International Journal of Electrical Power and Energy Systems*, 64, 2015 50–57. <https://doi.org/10.1016/j.ijepes.2014.07.033>
- [10] Newsom, C. Renewable Energy Potential in Nigeria: Low-carbon approaches to tackling Nigeria’s energy poverty. *International Institute for Environment and Development*, 2, 2012, 5-9
- [11] Saravanan, S., & Ramesh Babu, N. Analysis and implementation of a high step-up DC-DC converter for PV-based grid application. *Applied Energy*, 190, 2017 64–72. <https://doi.org/10.1016/j.apenergy.2016.12.094>
- [12] Sudhakar H. S., Indira M. S., Gujjala B. Balaraju and Siddhartha Bhatt M. *The Journal of CPRI*, Vol. 11, No. 1, March 2015 pp. 133-138.
- [13] Tseng, K., Huang, C., & Shih, W. A High Step-Up Converter With a Voltage Multiplier Module for a Photovoltaic System, 28(6), 2013, 3047–3057.
- [14] Veerachary M., Tomonobu S., Katsumi, U. Neural-network-based maximum-power-point tracking ofcoupled-inductor interleaved-boost-converter-supplied PV system using a fuzzy controller. *IEEE Trans Ind. Electron* 2003;50:749–58. Doi:10.1109/TIE.2003.814762